Journal of Medicinal Chemistry

Subscriber access provided by American Chemical Society

Article

Diketo Acid Pharmacophore. 2. Discovery of Structurally Diverse Inhibitors of HIV-1 Integrase

Raveendra Dayam, Tino Sanchez, and Nouri Neamati

J. Med. Chem., **2005**, 48 (25), 8009-8015• DOI: 10.1021/jm050837a • Publication Date (Web): 15 November 2005

Downloaded from http://pubs.acs.org on March 29, 2009

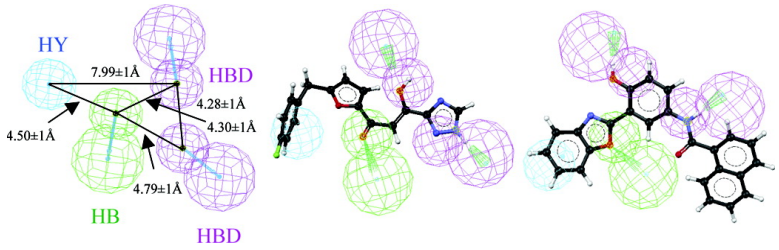

More About This Article

Additional resources and features associated with this article are available within the HTML version:

- Supporting Information
- Links to the 1 articles that cite this article, as of the time of this article download
- Access to high resolution figures
- Links to articles and content related to this article
- Copyright permission to reproduce figures and/or text from this article

View the Full Text HTML

ACS Publications
High quality. High impact.

Journal of Medicinal Chemistry is published by the American Chemical Society. 1155 Sixteenth Street N.W., Washington, DC 20036

Diketo Acid Pharmacophore. 2. Discovery of Structurally Diverse Inhibitors of HIV-1 Integrase

Raveendra Dayam, Tino Sanchez, and Nouri Neamati*

Department of Pharmaceutical Sciences, University of Southern California, School of Pharmacy, 1985 Zonal Avenue, PSC304, Los Angeles, California 90089

Received August 23, 2005

Because of its unique role in the viral replication process, HIV-1 integrase (IN) is an important antiretroviral drug target. The β-diketo acid class of IN inhibitors has played a major role in validating IN as a legitimate target for antiretroviral drug design. S-1360 (**1**) and L-870,810 (**2**) are examples of β-diketo acid related compounds to enter clinical trials. With an aim to discover novel lead compounds with diverse structural scaffolds, we employed common feature pharmacophore models using four known β-diketo acid analogues including S-1360 (*J. Med. Chem.* **2005**, *1*, 111−120). The best-ranked pharmacophore model (Hypo1) contained a hydrophobic (HYA), an H-bond acceptor (HBA), and two H-bond donor (HBD) features. A search of a 3D database containing ~150 000 small molecules using Hypo1 found 1700 compounds that satisfied all the features of the pharmacophore query. Of the 1700 compounds, 110 were selected for in vitro screening studies on the basis of their docking scores, predicted binding location inside the active site of IN, and their druglike properties. Forty-eight compounds inhibited IN catalytic activities with an IC_{50} value less than 100 μM. Twenty-seven structurally diverse inhibitors are reported here. Out of the 27 compounds, 13 compounds inhibited strand transfer activity of IN with an IC_{50} value less than 30 μM. These compounds are novel, druglike, and readily amenable for synthetic optimization.

Introduction

The pol gene of HIV-1 encodes three essential enzymes: reverse transcriptase (RT), protease (PR), and integrase (IN). Currently, 19 drugs are approved by the FDA for the treatment of HIV infection. These are targeted against RT, PR, and the viral entry process. IN plays a crucial role in the viral replication process by integrating the viral cDNA into the human genome.[1] Over the years, a plethora of IN inhibitors have been discovered.[2−5] Among all the reported IN inhibitors, the β-diketo acid class of compounds are the most promising and S-1360 (**1**) and L-870,810 (**2**) have entered clinical trials.[6−9] As more IN inhibitors are entering clinical trials, their safety, efficacy, and pharmacokinetic properties need to be optimized. Moreover, resistance to IN inhibitors are highly likely, and therefore, there is a need to develop second- and third-generation inhibitors.

Pharmacophore perception is one of the widely used analogue-based drug design methods where structural information of known lead compounds is utilized to identify novel and more potent compounds.[10−19] Previously, pharmacophore perception was successfully utilized in the discovery of several structurally diverse IN inhibitors using earlier leads.[20−25] Several structure-based pharmacophore models representing the dynamic nature of the IN active site were also generated and used to identify novel inhibitors.[26,27] Prior studies used pharmacophore techniques when no clinically validated drug was available to be used as a template. With the discovery of S-1360 as the first clinical candidate[6,28] the field of IN drug discovery has been gaining momentum. S-1360 and other selective IN inhibitors[8,9] have proven that IN is indeed "druggable", and the results with these drugs in primates and phase I clinical trials were very encouraging. Unfortunately, S-1360 failed phase II clinical trials because of pharmacokinetic problems and is no longer pursued as a viable drug. Because S-1360 is a highly selective IN inhibitor, it is possible to design compounds on the basis of its three-dimensional structure with entirely different pharmacokinetic profiles. We envisage that pharmacophore perception is an ideal approach for discovering second-generation IN inhibitors. In this study we expand on our recent report[25] using S-1360 as a template and present novel IN inhibitors with desirable predicted druglike properties.

Results and Discussion

To identify lead compounds with novel structural scaffolds and desired chemical features, we have generated common feature pharmacophore hypotheses using a training set consisting of four β-diketo acid-containing IN inhibitors. These include the clinical candidate S-1360 (**1**) (Figure 1).[25] Ten common feature pharmacophore hypotheses were generated using HipHop (Catalyst, version 4.8; Accelrys, Inc., 2003). The best-ranked pharmacophore hypothesis (Hypo1) was chosen for the database search and is shown in Figure 2A. The Hypo1 has four features and seven spheres, namely, a hydrophobic (HYA), an H-bond acceptor (HBA), and two H-bond donor (HBD) features (Figure 2A). The Hypo1 was used as a query to retrieve compounds that fit all

* To whom correspondence should be addressed. Phone: (323) 442-2341. Fax: (323) 442-1390. E-mail: neamati@usc.edu.

10.1021/jm050837a CCC: $30.25 © 2005 American Chemical Society
Published on Web 11/15/2005

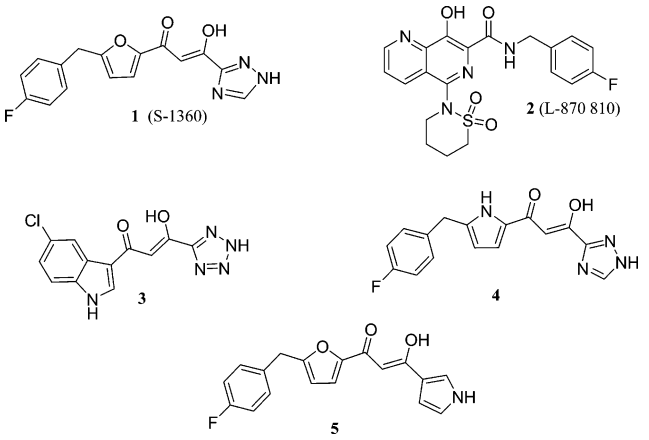

Figure 1. Structures of the HIV-1 IN inhibitors used in our training set.

the above features from a multiconformer 3D database of ~150 000 compounds. Compound **6**, one of the highly active compounds, was mapped onto the Hypo1 to provide understanding of the alignment of its chemical features with its pharmacophoric features (Figure 2C).

An earlier reported protocol for compound selection was also implemented in the present study.[25] All 1700 compounds retrieved from the database using Hypo1 were docked onto the active site of IN using the GOLD (genetic optimization for ligand docking) program to rank them on the basis of their ability to form favorable interactions with the IN active site (CCDC 2001, GOLD, version 1.2).[29,30] Finally, 110 compounds were selected for in vitro assays against purified IN on the basis of the GOLD score and the compounds' ability to chelate metal ion at the active site of IN and to satisfy Lipinski's rule of five. Of the 110 compounds tested against purified IN, 48 compounds inhibited IN with IC_{50} values ranging from 6 to 100 μM. Twenty-seven structurally diverse compounds with IN inhibitory activities are presented in this report.

In Vitro Inhibitory Activities of Novel Inhibitors of IN. IN inhibitory activities of all the compounds identified through the selection process were measured in an in vitro assay specific for IN. The chemical features of compounds **6**–**32** mapped by the pharmacophore features of Hypo1 are shown in Table 1. Blue represents a structural moiety mapped by the hydrophobic feature (HYA), and green and magenta represent functional groups mapped by the H-bond acceptor feature (HBA) and H-bond donor features (HBD), respectively (Table 1). Out of the 27 compounds presented in this report, 13 of them inhibited either the 3′-processing or the strand transfer activities of IN with an IC_{50} value less than 30 μM.

Compounds **6**–**9** share a benzoxazole and a free hydroxyl group in common. These molecules exhibited high to moderate IN inhibitory activities. Compound **10** containing a coumarin unit and a thiazole ring as its major structural components inhibited 3′-processing and strand transfer activities with IC_{50} values of 30 ± 4 and 10 ± 4 μM, respectively. Previously, several coumarin-based compounds containing more than one coumarin unit (dimers and tetramers) were reported as IN inhibitors.[31] Compound **11**, with a keto–enol moiety is a close analogue of linomide. It inhibited 3′-processing and strand transfer activities of IN with IC_{50} values of 40 ± 3 and 16 ± 6 μM, respectively. The keto–enol moiety is a commonly observed structural arrangement in the known IN inhibitors. Linomide, known to be an immunomodulator and an antineoplastic agent, also possesses the keto–enol moiety.[32,33]

Compounds **12** and **13** contain amide substituents at positions 2 and 5 of the core terephthalic acid inhibited 3′-processing activity with IC_{50} values of 9 ± 4 and 28 ± 12 μM, respectively, and strand transfer activity of IN with IC_{50} values of 7 ± 4 and 21 ± 9 μM, respectively. Compound **12**, with a phenylacetamide moiety, was more potent than compound **13**, which instead has a bulky naphthamide on the core terephthalic acid. Compound **14**, with an imidazole-5-carboxylate and a benzophenoneamide group, showed potent activity. It inhibited the 3′-processing and strand transfer activities of IN with IC_{50} values of 16 ± 8 and 17 ± 3 μM, respectively. The N-substituted tryptophan **15** is a moderate inhibitor of IN, and some of the structurally related molecules were reported previously as thrombin inhibitors.[34]

Compounds **16** and **17** both showed selectivity toward the inhibition of IN strand transfer activity. Compound **18** inhibited both the catalytic activities of IN with similar IC_{50} values. Compound **19** with a diketohydrazide as its major structural unit inhibited both catalytic activities but showed more potency against strand transfer activity of IN. Compound **20**, also containing a β-diketohydrazide moiety, inhibited strand transfer activity of IN with an IC_{50} value of 90 ± 10

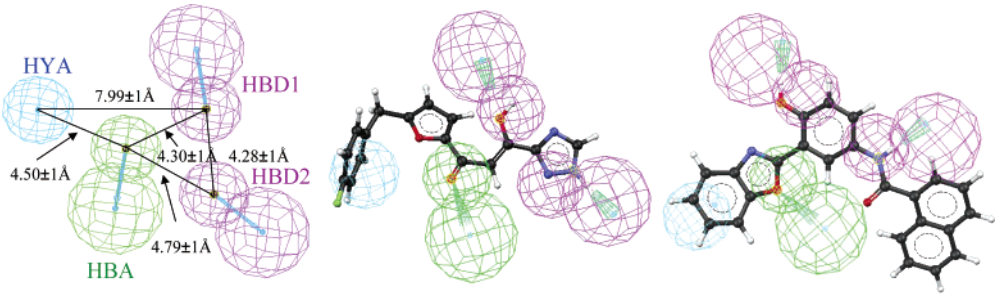

Figure 2. (A) Best-ranked HipHop generated pharmacophore hypothesis with four features (Hypo1). (B) S-1360 (**1**) is mapped onto Hypo1. Hypo1 was used in the database mining to identify novel HIV-1 integrase inhibitors. (C) A representative compound, **6**, is mapped on to Hypo1. The pharmacophoric features are shown as hydrophobic in light-blue (HYA), H-bond acceptor is shown in green (HBA), and H-bond donor is shown in magenta (HBD1-2).

Table 1. Inhibition of HIV-1 Integrase Catalytic Activities and GOLD Scores of a Set of Structurally Diverse Compounds Retrieved from the Database Using the Best Pharmacophore Hypo1

Compound	Structure	Inhibition of IN Catalytic Activities IC_{50} (μM)		GOLD Score
		3′-processing	Strand transfer	
6	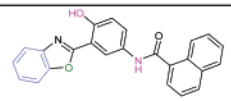	14±3	6±1	57.64
7	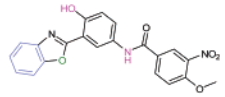	6±1	7	58.38
8	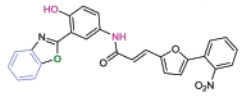	23±15	63±3	58.29
9	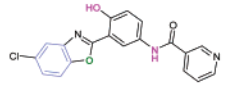	61±36	10±6	58.66
10	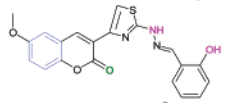	30±4	10±4	53.49
11	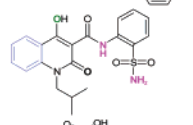	40±3	16±6	50.70
12	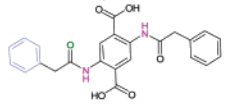	9±4	7±4	53.32
13	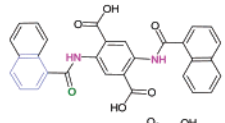	28±12	21±9	51.79
14	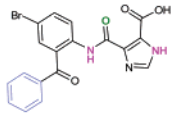	16±8	17±3	46.08
15	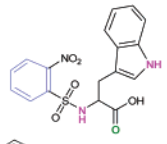	88±16	56±7	52.71
16	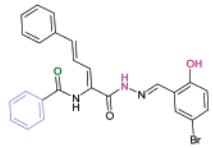	90±7	23±17	55.07
17	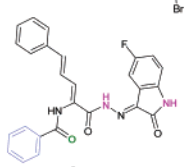	60±3	38±10	42.74
18	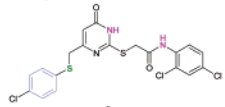	34±6	24±4	59.95
19	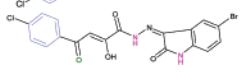	42±12	28±8	50.13
20	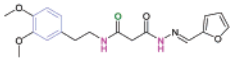	>100	90±10	51.77
21	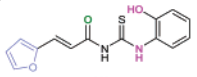	57±3	28±11	52.58
22	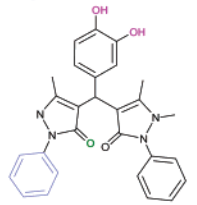	89±22	31±18	52.30
23	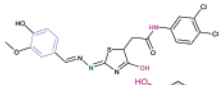	89	38	49.23
24	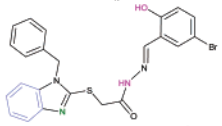	60±11	51±3	52.58
25	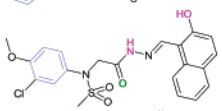	95±9	59±1	61.96
26	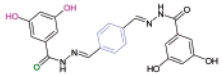	76±22	56±32	40.22
27	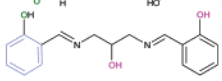	97±5	61±29	43.14
28	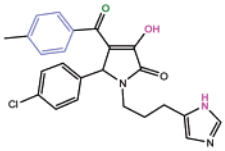	93±12	67±28	51.47
29	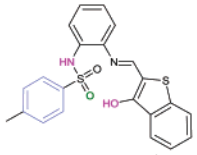	88±25	68±33	55.85
30	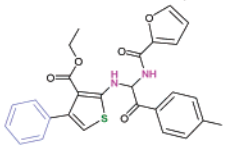	>100	79±44	61.77
31	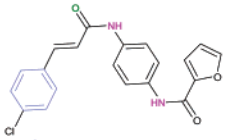	90±20	91±14	47.42
32	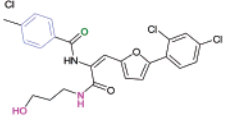	>1000	85±19	54.86

μM, but it did not inhibit the 3′-processing activity at 100 μM. Compounds **22**−**25**, all containing one or two free hydroxyl groups, showed moderate inhibitory activities against IN. The symmetric molecule **26**, with two 3,5-dihydroxy-*N*-methylenebenzohydrazide groups at positions 1 and 4 of the central phenyl ring, showed moderate activity against IN.

Compound **27**, a symmetric secondary alcohol with two salicylideneimino groups, showed moderate activity against IN. Several structurally related Schiff bases are known as metal chelaters. Compounds with molecular structures similar to that of compound **27** chelate manganese.[35] Compound **28**, with a highly substituted central butyrolactam ring and an imidazole group, is a

moderate inhibitor of IN. The Schiff base **29**, with a 3-hydroxybenzothiophene and a 4-methylbenzensulfonamide on the core phenyl ring, also showed moderate inhibitory activity against IN. Compounds **30** and **31**, both containing a 2-furancarboxamide group in common, are moderate inhibitors of IN. Compound **32**, with a free hydroxyl group, showed high selectivity toward the strand transfer activity of IN and was inactive against the 3′-processing activity of IN even at a tested concentration of 1000 μM.

Compounds **6**−**32**, with ample structural diversity, showed a wide range of inhibitory activities against both catalytic reactions of IN. Interestingly, most of these compounds possessed one or two free carboxylic or free hydroxyl groups, and some had a keto−enol arrangement. The keto−enol arrangement is a common structural feature found in many of the documented IN inhibitors. Compounds **11** and **19** containaing a keto−enol moiety showed significant inhibitory activity against IN. Owing to their novel structural features, several of these compounds provide potential leads for IN inhibitor design.

Because compounds **12** and **13** both contained two free carboxylate groups and showed considerable IN inhibitory activity, we investigated how the presence and arrangement of the two carbonyl oxygen atoms contribute to their inhibitory profile. These two carbonyl oxygen atoms are separated by five bonds (oxygen atoms in red and bonds in bold; see Table 2). Seven compounds with two carbonyl oxygen atoms separated by a five-bond distance were retrieved from the database and screened against IN. Compounds **33**−**35** have two carbonyl oxygen atoms arranged in a similar geometry. Compounds **33** and **34** showed significant inhibition against strand transfer activity of IN, while compound **35** was inactive at the highest tested concentration of 100 μM. A similar geometrical arrangement for the two carbonyl oxygen atoms is maintained to a large extent in **36**−**39**. However, they possessed diverse structural scaffolds. Interestingly, compounds **36**−**39** showed moderate inhibitory activity against IN. This indicates that the presence and geometry of the two carbonyl oxygen atoms separated by a five-bond distance could contribute to activity profile of the molecule. However, the relative geometry of the carbonyl groups in the molecule and their ability to participate and establish strong interactions within the IN active site are the key features for potency.

Antiviral Activity. Compounds **9**−**11** did not show any cytoprotection against HIV-1 infected CEM cells. Compound **12** with an EC_{50} value of 104 μM and CC_{50} value of >400 μM was confirmed as active in a cell-based antiviral assay. Unfortunately, compounds **16**−**24** showed significant cytotoxicity without antiviral activity.

Docking Studies. As part of the compound selection process, all the hits were docked onto the active site of IN. Most of the active compounds scored high GOLD fitness values. Some of the moderately active compounds **8**, **25**, **28**−**30**, and **32** also scored high GOLD fitness values. An example of the predicted bound conformation of one of the highly active compounds **6**, inside the IN active site, is shown in Figure 3 along with the crystallographically determined bound conformation of 5CITEP (**3**).[36] Compound **6** occupied a wide cavity surrounded by the active site amino acid residues Q62, D64, D116, P142, I151, E152, N155, K156, and K159. The hydroxyl group of compound **6** forms strong H-bonding interactions with the amino acid residues I151 and N155. The carbonyl oxygen atom of compound **6** involves an H-bonding interaction with amino acid residue Q62 (Table 3). The bound conformation of compound **6** inside the IN active site supports its inhibitory profile.

Table 2. Inhibition of HIV-1 Integrase Catalytic Activities by a Set of Compounds with Two Carbonyl Oxygen Atoms Separated by a Five-Bond Distance

Compound	Structure	Inhibition of IN Catalytic Activities IC_{50} (μM)	
		3'-processing	Strand transfer
33	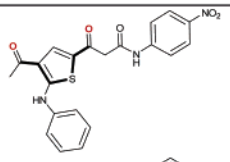	80±35	28±10
34	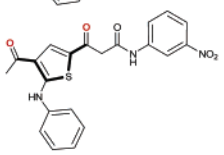	97±3	29±21
35	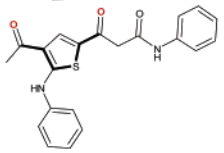	>100	>100
36	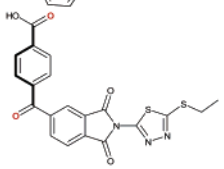	98±4	65±31
37	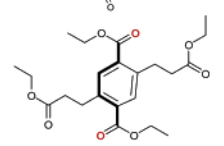	>100	94±10
38	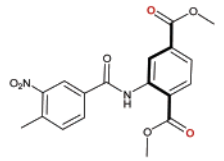	92±14	>100
39	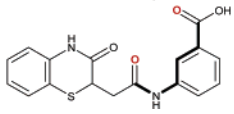	79±19	71±23

Conclusions

A set of novel IN inhibitors with diverse structural scaffolds were identified using a pharmacophore hypothesis that was generated on the basis of four known IN inhibitors including S-1360. Many of these compounds possess amenable chemical and structural features and will serve as potential leads for drug design strategies targeting IN. Further structural optimization to enhance IN inhibitory activity is in progress and will be reported in due course.

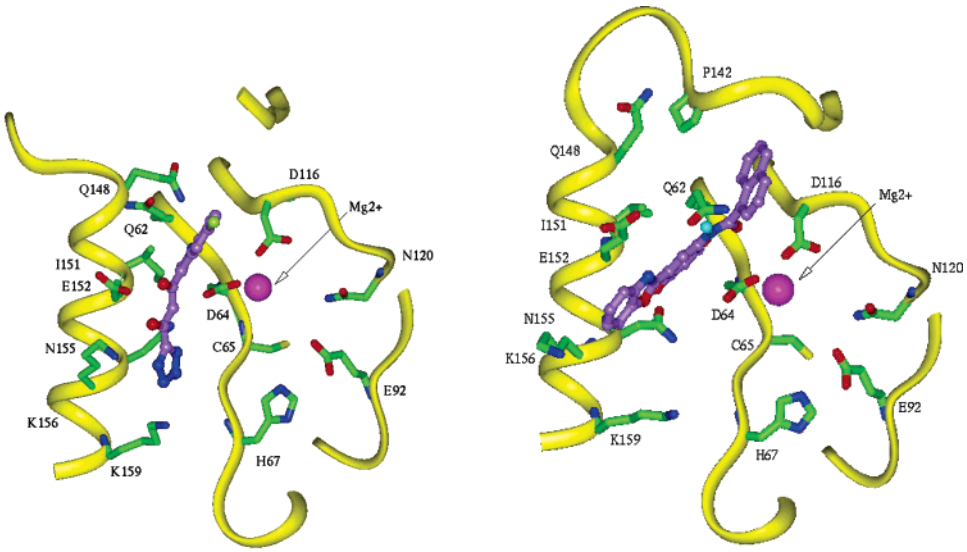

A **B**

Figure 3. (A) Crystallographically determined bound conformation of 5CITEP (PDB1QS4). (B) Predicted bound conformation of compound **6** inside the HIV-1 integrase active site. The ribbon model indicates the active site region, while the prominent active site amino acid residues are rendered as stick models. The violet ball-and-stick model represents compound **6**. The magenta sphere represents Mg^{2+}.

Table 3. H-bond Interactions and the Active Site Amino Acid Residues Interacting with Compound **6**

Compound **6**	
H-bond interactions[a]	Interacting amino acid residues
−OH···O=C N155 (1.61) −OH···O=C I151 (2.31)[b] −C=O···HN Q62 (1.81)	Q62, D64, D116, I151, E152, N155, K156

[a] The values in parentheses are H-bond distances in Å. [b] Backbone carbonyl of I151.

Experimental Section

Generation of Pharmacophore Hypotheses. Common feature pharmacophore hypotheses were generated using four β-diketo acid containing inhibitors (**1** and **3**− **5**) of IN (Figure 1). The structures and conformations of the four compounds were built within Catalyst on a multiprocessor Linux PC in parallel to a 24-CPU Silicon Graphics Onyx workstation as described.[37] The Poling algorithm implemented within Catalyst was used to generate conformations for all the compounds. For each compound all feasible unique conformations were generated over a 20 kcal/mol range using the BEST flexible conformation generation option in Catalyst. The Catalyst HipHop module was used to generate the common feature hypotheses.[25] HipHop evaluates a collection of conformational models of molecules and a selection of chemical features. The program then identifies configurations of features (pharmacophore) common to these molecules. The top-ranking pharmacophores are expected to identify the hypothetical orientation of the active compounds and the common binding features interacting with the target. All training set inhibitors were somewhat structurally diverse but possessed some common chemical features and comparable inhibitory potencies. On the basis of the structural information from these known inhibitors and the active site of IN, a set of features were selected to be present in the pharmacophore generation experiment. The chemical features considered in the pharmacophore model generation run were H-bond donor (HBD), H-bond acceptor (HBA), and hydrophobic aromatic (HYA). HipHop was forced to incorporate these features in the 10 top-ranking pharmacophore hypotheses generated.

Database Search. The highest ranked common feature pharmacophore was used as a search query to retrieve molecules with novel chemical structure and desired chemical features from an in-house multiconformer Catalyst-formatted database consisting of ∼150 000 compounds. The best flexible search databases/spread sheets method in Catalyst was used to search the database. Druglike properties of the retrieved hits from the database search were calculated using Accord for Excel (Accelrys, Inc.).

Docking. The subunit B of the core domain X-ray structure of IN (PDB code 1BIS) in which all the active site amino acid residues were resolved was chosen for our docking purpose. A Mg^{2+} ion was placed in the active site between carboxylate oxygen atoms of amino acid residues D64 and D116 based on the geometry of the Mg^{2+} ion that was present in the subunit A of IN in PDB 1BIS and subunit A in the IN-5CITEP complex X-ray structure (PDB 1QS4).[36] All the water molecules present in the protein were removed, and proper protonation states were assigned for acidic and basic residues of the protein. Docking was performed using version 1.2 of the GOLD (genetic optimization for ligand docking) software package. GOLD is an automated ligand docking program that uses a genetic algorithm to explore the full range of ligand conformational flexibility with partial flexibility of the receptor.[29] The algorithm was tested on a data set of over 300 complexes extracted from the Brookhaven Protein DataBank.[30] GOLD succeeded in more than 70% of the cases in reproducing the experimental bound conformation of the ligand. GOLD requires a user-defined binding site. It searches for a cavity within the defined area and considers all the solvent accessible atoms in the defined area as active site atoms. A 20 Å radius active site was defined considering the carboxylate oxygen (OD1) atom of residue D64 as the center of the active site. All the compounds retrieved by the pharmacophore model (Hypo 1) were docked into the active site of IN. On the basis of the GOLD fitness score, for each molecule a bound conformation with a high fitness score was considered as the best bound conformation. All docking runs were carried out using standard default settings with a population size of 100, a maximum number of 100 000 operations, and a mutation and crossover rate of 95. The fitness function that was implemented in GOLD consisted basically of H-bonding, complex energy, and ligand internal energy terms.

Materials, Chemicals, and Enzymes. All compounds were dissolved in DMSO, and stock solutions were stored at −20 °C. The γ-[^{32}P]-ATP was purchased from either Amersham Biosciences or ICN. The expression systems for wild-type IN and the soluble mutant $IN^{F185KC280S}$ were generous gifts of Dr. Robert Craigie, Laboratory of Molecular Biology, NIDDK, NIH, Bethesda, MD.

Preparation of Oligonucleotide Substrates. The oligonucleotides 21top, 5′-GTGTGGAAAATCTCTAGCAGT-3′, and 21bot, 5′-ACTGCTAGAGATTTTCCACAC-3′, were purchased from Norris Cancer Center Microsequencing Core Facility (University of Southern California) and purified by UV shadowing on polyacrylamide gel. To analyze the extent of 3′-processing and strand transfer using 5′-end-labeled substrates, 21top was 5′-end-labeled using T_4 polynucleotide kinase (Epicentre, Madison, WI) and γ-[^{32}P]-ATP (Amersham Biosciences or ICN). The kinase was heat-inactivated, and 21bot was added in 1.5 molar excess. The mixture was heated at 95 °C, allowed to cool slowly to room temperature, and run through a spin 25 minicolumn (USA Scientific) to separate annealed double-stranded oligonucleotide from unincorporated material.

Integrase Assays. To determine the extent of 3′-processing and strand transfer, wild-type IN was preincubated at a final concentration of 200 nM with the inhibitor in reaction buffer (50 mM NaCl, 1 mM HEPES, pH 7.5, 50 μM EDTA, 50 μM dithiothreitol, 10% glycerol (w/v), 7.5 mM $MnCl_2$, 0.1 mg/mL bovine serum albumin, 10 mM 2-mercaptoethanol, 10% dimethyl sulfoxide, and 25 mM MOPS, pH 7.2) at 30 °C for 30 min. Then, 20 nM of the 5′-end ^{32}P-labeled linear oligonucleotide substrate was added, and incubation was continued for an additional 1 h. Reactions were quenched by the addition of an equal volume (16 μl) of loading dye (98% deionized formamide, 10 mM EDTA, 0.025% xylene cyanol, and 0.025% bromophenol blue). An aliquot (5 μL) was electrophoresed on a denaturing 20% polyacrylamide gel (0.09 M Tris-borate, pH 8.3, 2 mM EDTA, 20% acrylamide, 8 M urea).

Gels were dried, exposed in a PhosphorImager cassette, analyzed using a Typhoon 8610 variable mode imager (Amersham Biosciences), and quantitated using ImageQuant 5.2. Percent inhibition (% I) was calculated using the following equation:

$$\% I = 100 \times \frac{1 - (D - C)}{N - C}$$

where C, N, and D are the fractions of a 21-mer substrate converted to 19-mer (3′-processing product) or strand transfer products for DNA alone, DNA plus IN, and IN plus drug, respectively. The IC_{50} values were determined by plotting the logarithm of drug concentration versus percent inhibition to obtain the concentration that produced 50% inhibition.

Anti-HIV Assays in Cultured Cells. The anti-HIV activity was evaluated in human T cell line CEM-SS infected with HIV-1 as described by Weislow et al.[38] In brief, cells were plated in 96-well plates at 5×10^3 cells/well and infected with $HIV\text{-}1_{RF}$ (MOI = 0.3). Serial dilutions of compounds were then immediately added to the cells in a final volume of 200 μL. In each experiment, AZT and dextran sulfate were included as control compounds for anti-HIV activity. The cells were maintained at 37 °C with 5% CO_2-containing humidified air for 6 days. Cell viability was quantified by absorbance at 450 nm after 4 h of incubation with 2,3-bis[2-methoxy-4-nitro-5-sulfophenyl]-5-[(phenylamino)carbonyl]-2*H*-tetrazolium hydroxide (XTT) at 0.2 mg/mL. Antiviral activity was graded on the basis of the degree of anti-HIV protection as active (80−100% protection), moderate (50−79% protection), and inactive (0−49% protection). Toxicity of the compounds was determined simultaneously on the same plate in uninfected CEM-SS cells.

Acknowledgment. This work was financially supported by funds from Gustavus and Louise Pfeiffer Research Foundation and by GlaxoSmithKline Drug Discovery and Development Award to Nouri Neamati.

References

(1) Brown, P. O. Integration. *Retroviruses*; Cold Spring Harbor Press: Cold Spring Harbor: Woodbury, NY, 1999; pp 161−203.
(2) Neamati, N. Patented small molecule inhibitors of HIV-1 integrase: a 10-year saga. *Expert Opin. Ther. Pat.* **2002**, *12*, 709−724.
(3) Dayam, R.; Neamati, N. Small-molecule HIV-1 integrase inhibitors: the 2001−2002 update. *Curr. Pharm. Des.* **2003**, *9*, 1789−1802.
(4) Gupta, S. P.; Nagappa, A. N. Design and development of integrase inhibitors as anti-HIV agents. *Curr. Med. Chem.* **2003**, *10*, 1779−1794.
(5) Pommier, Y.; Johnson, A. A.; Marchand, C. Integrase inhibitors to treat HIV/AIDS. *Nat. Rev. Drug Discovery* **2005**, *4*, 236−248.
(6) Yoshinaga, T. S.; Fujishita, T.; Fujiwara, T. In Vitro Activity of a New HIV-1 Integrase Inhibitor in Clinical Development. Presented at the 9th Conference on Retroviruses and Opportunistic Infections, Seattle, WA, 2002.
(7) Young, S. L-870,810: A Potent Antiviral HIV Integrase Inhibitor with Potential Clinical Utility. Presented at the XIV International AIDS Conference, West Point, PA, 2002.
(8) Hazuda, D. J.; Felock, P.; Witmer, M.; Wolfe, A.; Stillmock, K.; Grobler, J. A.; Espeseth, A.; Gabryelski, L.; Schleif, W.; Blau, C.; Miller, M. D. Inhibitors of strand transfer that prevent integration and inhibit HIV-1 replication in cells. *Science* **2000**, *287*, 646−650.
(9) Hazuda, D. J.; Young, S. D.; Guare, J. P.; Anthony, N. J.; Gomez, R. P.; Wai, J. S.; Vacca, J. P.; Handt, L.; Motzel, S. L.; Klein, H. J.; Dornadula, G.; Danovich, R. M.; Witmer, M. V.; Wilson, K. A.; Tussey, L.; Schleif, W. A.; Gabryelski, L. S.; Jin, L.; Miller, M. D.; Casimiro, D. R.; Emini, E. A.; Shiver, J. W. Integrase inhibitors and cellular immunity suppress retroviral replication in rhesus macaques. *Science* **2004**, *305*, 528−532.
(10) Milne, G. W.; Nicklaus, M. C.; Wang, S. Pharmacophores in drug design and discovery. *SAR QSAR Environ. Res.* **1998**, *9*, 23−38.
(11) Fang, X.; Wang, S. A Web-based 3D-database pharmacophore searching tool for drug discovery. *J. Chem. Inf. Comput. Sci.* **2002**, *42*, 192−198.
(12) Guner, O. F. *Pharmacophore Perception, Development, and Use in Drug Design*; International University Line: La Jolla, CA, 2000.
(13) Kurogi, Y.; Guner, O. F. Pharmacophore modeling and three-dimensional database searching for drug design using catalyst. *Curr. Med. Chem.* **2001**, *8*, 1035−1055.
(14) Langer, T.; Krovat, E. M. Chemical feature-based pharmacophores and virtual library screening for discovery of new leads. *Curr. Opin. Drug Discovery Dev.* **2003**, *6*, 370−376.
(15) Lengauer, T.; Lemmen, C.; Rarey, M.; Zimmermann, M. Novel technologies for virtual screening. *Drug Discovery Today* **2004**, *9*, 27−34.
(16) Lyne, P. D.; Kenny, P. W.; Cosgrove, D. A.; Deng, C.; Zabludoff, S.; Wendoloski, J. J.; Ashwell, S. Identification of compounds with nanomolar binding affinity for checkpoint kinase-1 using knowledge-based virtual screening. *J. Med. Chem.* **2004**, *47*, 1962−1968.
(17) Dror, O.; Shulman-Peleg, A.; Nussinov, R.; Wolfson, H. J. Predicting molecular interactions in silico: I. A guide to pharmacophore identification and its applications to drug design. *Curr. Med. Chem.* **2004**, *11*, 71−90.
(18) Patel, Y.; Gillet, V. J.; Bravi, G.; Leach, A. R. A comparison of the pharmacophore identification programs: Catalyst, DISCO and GASP. *J. Comput.-Aided Mol. Des.* **2002**, *16*, 653−681.
(19) van Drie, J. H. Pharmacophore discovery—lessons learned. *Curr. Pharm. Des.* **2003**, *9*, 1649−1664.
(20) Nicklaus, M. C.; Neamati, N.; Hong, H.; Mazumder, A.; Sunder, S.; Chen, J.; Milne, G. W.; Pommier, Y. HIV-1 integrase pharmacophore: discovery of inhibitors through three-dimensional database searching. *J. Med. Chem.* **1997**, *40*, 920−929.
(21) Neamati, N.; Hong, H.; Mazumder, A.; Wang, S.; Sunder, S.; Nicklaus, M. C.; Milne, G. W.; Proksa, B.; Pommier, Y. Depsides and depsidones as inhibitors of HIV-1 integrase: discovery of novel inhibitors through 3D database searching. *J. Med. Chem.* **1997**, *40*, 942−951.
(22) Hong, H.; Neamati, N.; Wang, S.; Nicklaus, M. C.; Mazumder, A.; Zhao, H.; Burke, T. R., Jr.; Pommier, Y.; Milne, G. W. Discovery of HIV-1 integrase inhibitors by pharmacophore searching. *J. Med. Chem.* **1997**, *40*, 930−936.
(23) Hong, H.; Neamati, N.; Winslow, H. E.; Christensen, J. L.; Orr, A.; Pommier, Y.; Milne, G. W. Identification of HIV-1 integrase inhibitors based on a four-point pharmacophore. *Antiviral Chem. Chemother.* **1998**, *9*, 461−472.
(24) Barreca, M. L.; Rao, A.; De Luca, L.; Zappala, M.; Gurnari, C.; Monforte, P.; De Clercq, E.; Van Maele, B.; Debyser, Z.; Witvrouw, M.; Briggs, J. M.; Chimirri, A. Efficient 3D database screening for novel HIV-1IN inhibitors. *J. Chem. Inf. Comput. Sci.* **2004**, *44*, 1450−1455.
(25) Dayam, R.; Sanchez, T.; Clement, O.; Shoemaker, R.; Sei, S.; Neamati, N. β-Diketo acid pharmacophore hypothesis. 1. Discovery of a novel class of HIV-1 integrase inhibitors. *J. Med. Chem.* **2005**, *48*, 111−120.

(26) Carlson, H. A.; Masukawa, K. M.; Rubins, K.; Bushman, F. D.; Jorgensen, W. L.; Lins, R. D.; Briggs, J. M.; McCammon, J. A. Developing a dynamic pharmacophore model for HIV-1 integrase. *J. Med. Chem*. **2000**, *43*, 2100−2114.
(27) Deng, J.; Lee, K. W.; Sanchez, T.; Cui, M.; Neamati, N.; Briggs, J. M. Dynamic receptor-based pharmacophore model development and its application in designing novel HIV-1 integrase inhibitors. *J. Med. Chem.* **2005**, *48*, 1496−1505.
(28) Billich, A. S-1360 Shionogi-GlaxoSmithKline. *Curr. Opin. Invest. Drugs* **2003**, *4*, 206−209.
(29) Jones, G.; Willett, P.; Glen, R. C.; Leach, A. R.; Taylor, R. Development and validation of a genetic algorithm for flexible docking. *J. Mol. Biol.* **1997**, *267*, 727−748.
(30) Nissink, J. W.; Murray, C.; Hartshorn, M.; Verdonk, M. L.; Cole, J. C.; Taylor, R. A new test set for validating predictions of protein−ligand interaction. *Proteins* **2002**, *49*, 457−471.
(31) Zhao, H.; Neamati, N.; Hong, H.; Mazumder, A.; Wang, S.; Sunder, S.; Milne, G. W.; Pommier, Y.; Burke, T. R., Jr. Coumarin-based inhibitors of HIV integrase. *J. Med. Chem.* **1997**, *40*, 242−249.
(32) Tarkowski, A.; Gunnarsson, K.; Stalhandske, T. Effects of LS-2616 administration upon the autoimmune disease of (NZB × NZW) F1 hybrid mice. *Immunology* **1986**, *59*, 589−594.
(33) Bergh, J. C.; Totterman, T. H.; Termander, B. C.; Strandgarden, K. A.; Gunnarsson, P. O.; Nilsson, B. I. The first clinical pilot study of roquinimex (Linomide) in cancer patients with special focus on immunological effects. *Cancer Invest.* **1997**, *15*, 204−211.
(34) Jean, A. K.; Thomas, T.; David, B.; Paul, H.; Kurt, H.; Beat, W.; Ludvik, L.; Gerard, S.; Kalus, G.; Peter, W. H. *Guanidine Derivatives. Compositions and Use*; Hoffmann La Roche: Nutley, NJ, 1993.
(35) Gelasco, A.; Pecoraro, V. L. [Mn(III)(2-OHsalpn)]2 is an efficient functional-model for the manganese catalases. *J. Am. Chem. Soc.* **1993**, *115*, 7928−7929.
(36) Goldgur, Y.; Craigie, R.; Cohen, G. H.; Fujiwara, T.; Yoshinaga, T.; Fujishita, T.; Sugimoto, H.; Endo, T.; Murai, H.; Davies, D. R. Structure of the HIV-1 integrase catalytic domain complexed with an inhibitor: a platform for antiviral drug design. *Proc. Natl. Acad. Sci. U.S.A.* **1999**, *96*, 13040−13043.
(37) Long, Y. Q.; Jiang, X. H.; Dayam, R.; Sanchez, T.; Shoemaker, R.; Sei, S.; Neamati, N. Rational design and synthesis of novel dimeric diketoacid-containing inhibitors of HIV-1 integrase: Implication for binding to two metal ions on the active site of integrase. *J. Med. Chem.* **2004**, *47*, 2561−2573.
(38) Weislow, O. W.; Kiser, R.; Fine, D.; Bader, J.; Shoemaker, R. H.; Boyd, M. R. New soluble-formazan assay for HIV-1 cytopathic effects: application to high-flux screening of synthetic and natural products for AIDS antiviral activity. *J. Natl. Cancer Inst.* **1989**, 81, 577−586.

JM050837A